

Ground states of a frustrated spin- $\frac{1}{2}$ antiferromagnet: Cs_2CuCl_4 in a magnetic field

M. Y. Veillette,¹ J. T. Chalker,¹ and R. Coldea²¹*Theoretical Physics, University of Oxford, 1, Keble Road, Oxford, OX1 3NP, United Kingdom*²*Oxford Physics, Clarendon Laboratory, Parks Road, Oxford OX1 3PU, United Kingdom*

(Received 18 January 2005; published 29 June 2005)

We present detailed calculations of the magnetic ground state properties of Cs_2CuCl_4 in an applied magnetic field, and compare our results with recent experiments. The material is described by a spin Hamiltonian, determined with precision in high field measurements, in which the main interaction is antiferromagnetic Heisenberg exchange between neighboring spins on an anisotropic triangular lattice. An additional, weak Dzyaloshinskii-Moriya interaction introduces easy-plane anisotropy, so that behavior is different for transverse and longitudinal field directions. We determine the phase diagram as a function of field strength for both field directions at zero temperature, using a classical approximation as a first step. Building on this, we calculate the effect of quantum fluctuations on the ordering wave vector and components of the ordered moments, using both linear spinwave theory and a mapping to a Bose gas which gives exact results when the magnetization is almost saturated. Many aspects of the experimental data are well accounted for by this approach.

DOI: 10.1103/PhysRevB.71.214426

PACS number(s): 75.10.Jm, 75.25.+z, 75.40.Gb

I. INTRODUCTION

The layered, insulating magnet Cs_2CuCl_4 has attracted intense recent experimental and theoretical attention.¹⁻¹¹ Much of the interest arises because the material is a rare example of a spin $S=\frac{1}{2}$, triangular lattice antiferromagnet.²⁻⁴ Its small spin, quasi-two-dimensionality, and geometric frustration are all features expected to enhance zero-point fluctuations in Néel-ordered states and to promote spin-liquid states.¹²⁻¹⁴ Indeed, inelastic neutron scattering experiments on Cs_2CuCl_4 ⁴ have revealed extended scattering continua in the dynamic structure factor, and various spin liquid states^{7,9,11} have been proposed to explain this observation in terms of fractionalized excitations. Nevertheless, at sufficiently low temperature Cs_2CuCl_4 displays conventional, magnetically ordered states over much of the phase diagram spanned by magnetic field strength and direction.¹⁻⁴ In this paper, we develop a theoretical treatment of these ordered states using two approaches. Starting from a classical description, we discuss fluctuations using linear spinwave theory. And starting from the fully polarized spin state reached at high field, we discuss fluctuations as a dilute Bose gas of spin flips. We present a detailed comparison of our results with experiment.

The low-temperature states of Cs_2CuCl_4 have been examined as a function of magnetic field strength and direction, using neutron diffraction.^{2,3} At zero field, long-range order, in the form of an incommensurate spiral spin structure, occurs below a Néel temperature of $T_N=0.62$ K. The magnetic moments lie in an easy plane due to anisotropy arising from a Dzyaloshinskii-Moriya interaction. The presence of this interaction, breaking $\text{SU}(2)$ symmetry in the spin Hamiltonian, has profound consequences for the behavior of the system in a magnetic field, and the ordering observed depends on the field direction.² Two field directions have been studied: *transverse* to the easy plane (along the crystallographic a direction) and *longitudinal*—within the easy plane (the crystallographic b - c plane). In a transverse field, spins cant out of the easy plane towards the field direction, gaining Zeeman

energy. Below a critical field of $B_{cr}^a=8.44$ T, ordered moments at different sites lie on a cone around the field direction. As the critical field is approached the cone angle closes to zero, and above it the magnetization is saturated. The behavior for a longitudinal magnetic field is considerably more complex.^{2,5} For fields along the c axis of strength B^c , at weak fields, $B^c < 1.4$ T, the anisotropy confines the spins in the b - c plane, creating a distorted cycloid. In the field range $1.4 \text{ T} < B^c < 2.1$ T, a second incommensurately ordered phase appears. At intermediate field strengths, in the range $2.1 \text{ T} < B^c < 7.1$ T, no magnetic Bragg peaks have so far been reported. In stronger fields, magnetic Bragg peaks⁵ at incommensurate wave vector are found up to the critical field $B_{cr}^c=8.0$ T, beyond which the magnetization is saturated at low temperature.

In this article our starting point is the spin Hamiltonian for Cs_2CuCl_4 , as determined by high-field experiments.³ We discuss the symmetry of this Hamiltonian and establish its ground-state phase diagram in transverse and longitudinal fields, within a classical approximation. We find incommensurate phases of three types. Extending our treatment to include quantum fluctuations, we proceed in two ways. First, we set out linear spinwave theory, treating fluctuations around the classical state at leading order using a standard $1/S$ expansion. Although the expansion parameter is not small in the case at hand, results known for the nearest neighbor Heisenberg antiferromagnet on the square^{15,16} and isotropic triangular¹⁷ lattices suggest that linear spinwave theory is likely to be quite accurate even for $S=\frac{1}{2}$. Second, supplementing the $1/S$ expansion, we apply theory for a dilute Bose gas to spin flips in a system with almost saturated magnetization. Using both methods, we determine quantum corrections to the ordering wave vector and components of the local ordered moments as a function of field strength. The results depend markedly on the presence of a Dzyaloshinskii-Moriya interaction and on the orientation of the applied magnetic field. We also investigate the effect of interlayer exchange, focusing on its influence on magnetic

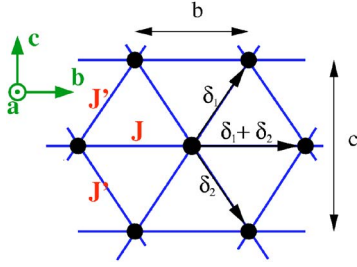


FIG. 1. (Color online) The magnetic sites and exchange couplings within a single layer of Cs_2CuCl_4 . Layers are stacked along the a direction, with interlayer spacing $a/2$ and a relative displacement in the c -direction.

order in a transverse field. We compare our results extensively with experimental data.

The remainder of the paper is organized as follows. We introduce the spin Hamiltonian and discuss its symmetries in Sec. II. In Sec. III, we develop classical theory and establish the phase diagram within a classical approximation, in transverse and longitudinal fields. We examine the effects of quantum fluctuations using the $1/S$ expansion and dilute Bose gas methods in Sec. IV, calculating static properties and comparing these with experimental data. In Sec. V we consider interlayer coupling. Finally, in Sec. VI, we summarize our conclusions.

II. CRYSTAL STRUCTURE AND SPIN HAMILTONIAN

The magnetic moments in Cs_2CuCl_4 are carried by Cu^{2+} ions. The orthorhombic unit cell contains four CuCl_4^{2-} tetrahedra arranged in two layers in the b - c plane.⁴ The location of magnetic sites within a single layer is illustrated in Fig. 1. Exchange interactions are sufficiently weak that it is possible using laboratory magnetic fields to fully polarize the moments at low temperature, and the spin Hamiltonian has been determined from a study of the excitation spectrum in a saturating transverse field.³ This method has the advantage of yielding interaction constants with the minimum of theoretical assumptions, since it focuses on the dynamics of single spin flips. In this way it has been established that the largest interaction is antiferromagnetic exchange J , coupling neighboring spins along the chains, and that neighbors on adjacent chains have a weaker exchange coupling J' . In addition, the measurements indicate a Dzyaloshinskii-Moriya (DM) exchange between chains, allowed by symmetry,¹⁸ and a weak antiferromagnetic nearest-neighbor interlayer coupling J'' , which stabilizes long-range magnetic order against thermal fluctuations.

The model Hamiltonian, with experimentally determined parameter values given in Table I, is

$$\mathcal{H} = \mathcal{H}_0 + \mathcal{H}_{DM} + \mathcal{H}_B, \quad (1)$$

where \mathcal{H}_0 is the Heisenberg exchange energy, \mathcal{H}_{DM} represents the DM interaction, and \mathcal{H}_B is the Zeeman energy in an applied magnetic field. Denoting spin- $\frac{1}{2}$ operators at the sites \mathbf{R} of a stacked anisotropic triangular lattice by $\mathbf{S}_{\mathbf{R}}$, the exchange energy is

TABLE I. Hamiltonian parameters, from Ref. 3.

Parameters	Experiment
J (meV)	0.374(5)
J' (meV)	0.128(5)
J'' (meV)	0.017(2)
D (meV)	0.020(2)

$$\mathcal{H}_0 = \sum_{\mathbf{R}} [J \mathbf{S}_{\mathbf{R}} \cdot \mathbf{S}_{\mathbf{R}+\delta_1+\delta_2} + J' (\mathbf{S}_{\mathbf{R}} \cdot \mathbf{S}_{\mathbf{R}+\delta_1} + \mathbf{S}_{\mathbf{R}} \cdot \mathbf{S}_{\mathbf{R}+\delta_2}) + J'' \mathbf{S}_{\mathbf{R}} \cdot \mathbf{S}_{\mathbf{R}+\delta_3}], \quad (2)$$

where the nearest neighbor vectors δ_1 and δ_2 are indicated in Fig. 1 and the out-of-plane vector δ_3 connects spins on adjacent layers. The DM energy is

$$\mathcal{H}_{DM} = - \sum_{\mathbf{R}} (-1)^n \mathbf{D} \cdot \mathbf{S}_{\mathbf{R}} \times (\mathbf{S}_{\mathbf{R}+\delta_1} + \mathbf{S}_{\mathbf{R}+\delta_2}), \quad (3)$$

where $\mathbf{D} = (D, 0, 0)$ is a vector associated with the oriented bond between the two coupled spins and n is a layer index. The factor $(-1)^n$ indicates that the interaction alternates between even and odd layers, which are inverted versions of one another. The Zeeman energy arising from a magnetic field $\mathbf{B} = (B^a, B^b, B^c)$ is

$$\mathcal{H}_B = - \sum_{\mathbf{R}} g_i \mu_B B^i S_{\mathbf{R}}^i, \quad (4)$$

where g is the gyromagnetic tensor $g = (2.20, 2.08, 2.30)$.¹⁹

We omit the dipole-dipole interaction and several small effects, including a relative offset of the Cu ions along c between adjacent layers, a small component of the \mathbf{D} vector perpendicular to the a axis and possible anisotropy of the exchange interactions in spin space.

At the classical level, the intrachain coupling J favors a staggered magnetization in the spin chains and the interchain coupling J' frustrates this state. As J'/J is varied, \mathcal{H}_0 interpolates between the fully frustrated Hamiltonian for the isotropic triangular lattice ($J'=J$) and that for uncoupled one-dimensional spin chains ($J'=0$). The DM interaction favors states in which spins lie in the b - c plane, with a rotation of $\pi/2$ between adjacent spin chains.

It is convenient at this point to introduce notation associated with reciprocal space. We express wave vectors in terms of the reciprocal lattice vectors, writing $\mathbf{Q} = (h, k, l)$ as shorthand for $2\pi(h/a, k/b, l/c)$. The Fourier transforms of the exchange and DM interactions are

$$J_{\mathbf{Q}} = J \cos(2\pi k) + 2J' \cos(\pi k) \cos(\pi l) \quad (5)$$

and

$$D_{\mathbf{Q}} = -2D \sin(\pi k) \cos(\pi l). \quad (6)$$

When considering transverse magnetic fields, these appear in the combination

$$J_{\mathbf{Q}}^T = J_{\mathbf{Q}} + D_{\mathbf{Q}}. \quad (7)$$

We close this section with a discussion of the symmetry of the Hamiltonian \mathcal{H} . While \mathcal{H}_0 has full SU(2) spin symmetry, \mathcal{H}_{DM} has a lower, $\mathbb{Z}_2 \otimes \text{U}(1)$ symmetry. Here, U(1) arises from spin rotations around the \mathbf{D} vector, and \mathbb{Z}_2 originates from invariance under the combination of space inversion ($\mathbf{R} \rightarrow -\mathbf{R}$) and the spin operations

$$\begin{aligned} \mathbf{S} \times \hat{\mathbf{x}} &\rightarrow -\mathbf{S} \times \hat{\mathbf{x}}, \\ \mathbf{S} \cdot \hat{\mathbf{x}} &\rightarrow \mathbf{S} \cdot \hat{\mathbf{x}}, \end{aligned} \quad (8)$$

where $\hat{\mathbf{x}}$ is an arbitrary unit vector in the b - c plane. To illustrate the nature of the \mathbb{Z}_2 symmetry, one can consider the chiral scalar $K = \sum_{\Delta} \mathbf{S}_1 \cdot (\mathbf{S}_2 \times \mathbf{S}_3)$, where the spin product is performed in a cyclical fashion over all triangular plaquettes. Under the \mathbb{Z}_2 operation, $\mathcal{H}_0 + \mathcal{H}_{DM}$ is invariant but $K \rightarrow -K$. The inclusion of \mathcal{H}_B further reduces the symmetry, to U(1) in a transverse magnetic field (with S^a a conserved quantity), and to \mathbb{Z}_2 in a longitudinal field.

III. CLASSICAL ANALYSIS

The classical approximation consists of treating the spin operators \mathbf{S} as classical vectors of length $S = \frac{1}{2}$. The Hamiltonian then becomes an energy functional that can be minimized to determine the magnetic structure. Omitting interlayer exchange and DM interactions, the classical ground state in zero field is a spin spiral

$$\mathbf{S}_{\mathbf{R}} = S \begin{pmatrix} 0 \\ \cos(\mathbf{Q}_{cl}^* \cdot \mathbf{R} + \alpha) \\ \sin(\mathbf{Q}_{cl}^* \cdot \mathbf{R} + \alpha) \end{pmatrix}, \quad (9)$$

where the arbitrary phase α reflects spontaneous breaking of the U(1) symmetry and the wave vector \mathbf{Q}_{cl}^* is determined by minimizing the exchange energy $J_{\mathbf{Q}}$. We find $\mathbf{Q}_{cl}^* = \pm(0, \frac{1}{2} + \epsilon_{cl}^*, 0)$ where $\epsilon_{cl}^* = \pi^{-1} \arcsin(J'/2J) = 0.0547$.

With \mathcal{H}_{DM} included, the degeneracy of the ground state with respect to the sign of the ordering wave vector is broken. Since the sign of the DM term alternates on adjacent layers, the direction of the wave vector alternates from layer to layer to give the spin structure (setting $\alpha = 0$)

$$\mathbf{S}_{\mathbf{R}} = S \begin{pmatrix} 0 \\ \cos(\mathbf{Q}_{cl} \cdot \mathbf{R}) \\ (-1)^n \sin(\mathbf{Q}_{cl} \cdot \mathbf{R}) \end{pmatrix}, \quad (10)$$

where now \mathbf{Q}_{cl} is determined by the minimum of $J_{\mathbf{Q}}^T$. We find $\mathbf{Q}_{cl} = (0, \frac{1}{2} + \epsilon_{cl}, 0)$ with $\epsilon_{cl} = 0.0533$.

The classical ground state in the presence of a transverse magnetic field can be found easily because U(1) symmetry ensures that only Fourier components with $\mathbf{Q} = \mathbf{0}$ and $\mathbf{Q} = \mathbf{Q}_{cl}$ contribute to the spin configuration. The spiral order of spin components within the b - c plane is preserved, and the spins cant towards the field direction to produce a cone state with

$$\mathbf{S}_{\mathbf{R}} = S \begin{pmatrix} \sin \theta_0 \\ \cos \theta_0 \cos(\mathbf{Q}_{cl} \cdot \mathbf{R}) \\ (-1)^n \cos \theta_0 \sin(\mathbf{Q}_{cl} \cdot \mathbf{R}) \end{pmatrix}, \quad (11)$$

where, measuring magnetic field in the reduced units $h^i = g^i \mu_b B^i / S$, $\sin \theta_0 = h^a / h_{cr}^a$. The critical field in reduced units is $h_{cr}^a = 2(J_0^T - J_{\mathbf{Q}}^T)$, giving $B_{cr}^a = 8.36$ T. The same expression for B_{cr}^a also emerges from an exact treatment of the quantum Hamiltonian for a single layer (see Ref. 3 and Sec. IV B); the small difference between this value and the experimental one³ of 8.44 T is partly due to interlayer exchange (see Sec. V). At higher fields, the spins are fully polarized along the field direction.

Ground states in a longitudinal field are considerably more complex because the magnetic field breaks U(1) symmetry and many Fourier harmonics contribute to the spin configuration. A useful guide to the behavior one should expect is provided by results for frustrated magnetic systems in a magnetic field, with single ion anisotropy rather than DM interactions. In that case, if anisotropy is weak, there is a first-order transition between a distorted cycloid state at low field, in which spins are confined to the easy plane, and an incommensurate cone structure with its axis along the field direction at high field.²⁰

To investigate such phenomena in the problem we are concerned with, we have studied spin configurations obtained by minimizing the classical energy functional numerically. We use periodic boundary conditions with a period of over 1000 sites in the b direction, and have examined many minima for a range of values of longitudinal fields. We find two phases separated by a first-order transition. For $h/h_{cr} < 0.35$, the zero-field spin spiral evolves smoothly into a distorted cycloid in which spins lie in the b - c plane. This state has a continuous degeneracy associated with phason modes.²¹ For fields in the range $0.35 < h/h_{cr} < 1$, an incommensurate out-of-plane solution is optimal. It has a nonzero value for the chiral scalar K and therefore breaks \mathbb{Z}_2 symmetry. A very good approximation to the out-of-plane numerical solution is provided by the expression

$$\mathbf{S}_{\mathbf{R}} = S \begin{pmatrix} \cos \theta_0 \cos(\mathbf{Q} \cdot \mathbf{R}) \cos \eta + \sin \theta_0 \sin \eta \\ (-1)^n \cos \theta_0 \sin(\mathbf{Q} \cdot \mathbf{R}) \\ \sin \theta_0 \cos \eta - \cos \theta_0 \cos(\mathbf{Q} \cdot \mathbf{R}) \sin \eta \end{pmatrix}. \quad (12)$$

In this approximation, only the Fourier components $\mathbf{0}$ and \mathbf{Q} appear, and the ordering wave vector is within a few percent of \mathbf{Q}_{cl}^* . Spin directions at different sites form a cone, which has a height $S \sin \theta_0$ and an axis lying in the a - c plane, tilted at an angle η to the c -direction. Moving from site to site in the b -direction, the spin projection onto the easy plane traces out an ellipse. The eccentricity of this ellipse is associated with a nonzero DM energy, and $\eta \propto D$ for small D . A second ground state, related by \mathbb{Z}_2 symmetry to the first, is generated by the operation: $\mathbf{Q} \rightarrow -\mathbf{Q}$ and $\eta \rightarrow -\eta$.

In spite of the proximity of the incommensurate wave vector to the commensurate value $(0, \frac{1}{2}, 0)$, the commensurate states are found to be well separated in energy from the incommensurate solutions, within a classical treatment.

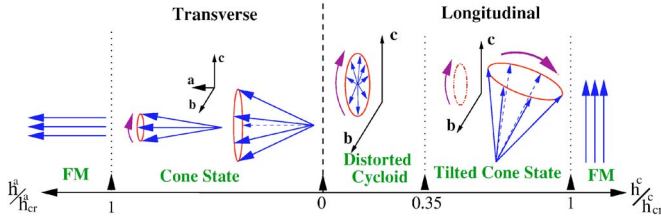


FIG. 2. (Color online) The phase diagram in the classical limit, with a schematic representation of the different phases. Transitions between the cone states and the ferromagnetic states are second order. The distorted cycloid and the tilted cone states are separated by a first-order transition.

The results of this classical analysis are summarized in Fig. 2. Behavior in a transverse field is in qualitative agreement with the experimental findings outlined in Sec. I. We delay a quantitative comparison between theory and experiment until after our discussion of the effects of quantum fluctuations in Sec. IV. Contrastingly, observed behavior in a longitudinal field shows different features from the classical phase diagram. In particular, the state found in the field range $2.1 \text{ T} < B^c < 7.1 \text{ T}$ does not appear classically.

IV. QUANTUM FLUCTUATIONS

The classical ground states determined in Sec. III provide a starting point for a treatment of quantum fluctuations. This can be approached using either a $1/S$ expansion, or directly for $S = \frac{1}{2}$ by expanding in powers of the density of reversed spins in a polarized background, viewing these as a dilute Bose gas. While the $1/S$ expansion is uncontrolled when applied to Cs_2CuCl_4 , it is known to produce quite accurate results for some simpler two-dimensional $S = \frac{1}{2}$ systems.^{15–17} Conversely, the density of reversed spins is controlled by field strength and the expansion parameter is $(1 - h/h_{cr})$. It is worth pointing out that quantum fluctuations in Cs_2CuCl_4 do not break a classical degeneracy, as is the case for the isotropic triangular lattice antiferromagnets in a field,²² but are likely to have substantial quantitative effects on ground state properties.

A. Large S -expansion

We now turn to a description of the calculations. The procedure is standard: starting from a classical, ordered state we use the Holstein-Primakoff transformation to obtain a bosonic Hamiltonian.^{23–29} Considering only the quadratic part of this Hamiltonian, we obtain the leading quantum contribution in a $1/S$ expansion.

1. Transverse field

In a transverse magnetic field, the classical ground state is an incommensurately ordered spin cone with wave vector \mathbf{Q} , given by Eq. (11). We introduce a rotating coordinate system in spin space via

$$\begin{pmatrix} S_{\mathbf{R}}^a \\ S_{\mathbf{R}}^b \\ S_{\mathbf{R}}^c \end{pmatrix} = \begin{pmatrix} 1 & 0 & 0 \\ 0 & \cos(\mathbf{Q} \cdot \mathbf{R}) & -(-)^n \sin(\mathbf{Q} \cdot \mathbf{R}) \\ 0 & (-)^n \sin(\mathbf{Q} \cdot \mathbf{R}) & \cos(\mathbf{Q} \cdot \mathbf{R}) \end{pmatrix} \times \begin{pmatrix} \cos \theta & 0 & \sin \theta \\ 0 & 1 & 0 \\ -\sin \theta & 0 & \cos \theta \end{pmatrix} \begin{pmatrix} S_{\mathbf{R}}^x \\ S_{\mathbf{R}}^y \\ S_{\mathbf{R}}^z \end{pmatrix}, \quad (13)$$

chosen so that the z axis at each site is aligned with the classical spin direction. A central objective of this section is to calculate quantum corrections to classical values of the ordering wave vector \mathbf{Q} and the canting angle θ . We omit the small interlayer exchange J'' , postponing a discussion of some of its effects to Sec. V.

The Holstein-Primakoff transformation is

$$S_{\mathbf{R}}^x = \frac{\sqrt{2S}}{2} (\phi_{\mathbf{R}}^\dagger + \phi_{\mathbf{R}}),$$

$$S_{\mathbf{R}}^y = i \frac{\sqrt{2S}}{2} (\phi_{\mathbf{R}}^\dagger - \phi_{\mathbf{R}}),$$

$$S_{\mathbf{R}}^z = S - \phi_{\mathbf{R}}^\dagger \phi_{\mathbf{R}}, \quad (14)$$

where the boson creation and annihilation operators satisfy the commutation relation $[\phi_{\mathbf{R}}, \phi_{\mathbf{R}'}^\dagger] = \delta_{\mathbf{R}, \mathbf{R}'}$. Introducing the Fourier transform

$$\phi_{\mathbf{k}}^\dagger = \frac{1}{\sqrt{N}} \sum_{\mathbf{R}} \phi_{\mathbf{R}}^\dagger e^{-i\mathbf{k} \cdot \mathbf{R}}, \quad (15)$$

for a lattice of N sites, the Hamiltonian of Eq. (1) takes the form

$$\mathcal{H} = \mathcal{H}_0 + \mathcal{H}_1 + \mathcal{H}_2 + \dots, \quad (16)$$

where \mathcal{H}_n is proportional to $S^{2-n/2}$ and consists of products of n normal-ordered boson operators. The leading terms are

$$\mathcal{H}_0 = NS^2 [J_{\mathbf{Q}}^T + (J_0^T - J_{\mathbf{Q}}^T) \sin^2 \theta - h^a \sin \theta],$$

$$\mathcal{H}_1 = \sqrt{\frac{NS^3}{2}} \cos \theta [2(J_0^T - J_{\mathbf{Q}}^T) \sin \theta - h^a] (\phi_0^\dagger + \phi_0),$$

$$\begin{aligned} \mathcal{H}_2 = NS & \left(J_{\mathbf{Q}}^T + (J_0^T - J_{\mathbf{Q}}^T) \sin^2 \theta - \frac{h^a}{2} \sin \theta \right) \\ & + S \sum_{\mathbf{k}} (A_{\mathbf{k}} + C_{\mathbf{k}}) (\phi_{\mathbf{k}}^\dagger \phi_{\mathbf{k}} + \phi_{\mathbf{k}} \phi_{\mathbf{k}}^\dagger) \\ & + B_{\mathbf{k}} (\phi_{-\mathbf{k}}^\dagger \phi_{\mathbf{k}}^\dagger + \phi_{-\mathbf{k}} \phi_{\mathbf{k}}), \end{aligned} \quad (17)$$

where the sum on \mathbf{k} is performed over the first Brillouin zone and

$$\begin{aligned}
A_{\mathbf{k}} &= \frac{1}{4}(2J_{\mathbf{k}} + J_{\mathbf{Q}+\mathbf{k}}^T + J_{\mathbf{Q}-\mathbf{k}}^T) - J_{\mathbf{Q}}^T - \frac{1}{4}(2J_{\mathbf{k}} - J_{\mathbf{Q}+\mathbf{k}}^T - J_{\mathbf{Q}-\mathbf{k}}^T)\sin^2 \theta \\
&\quad - (J_0^T - J_{\mathbf{Q}}^T)\sin^2 \theta + \frac{h^a}{2} \sin \theta, \\
B_{\mathbf{k}} &= \frac{1}{4}(2J_{\mathbf{k}} - J_{\mathbf{Q}+\mathbf{k}}^T - J_{\mathbf{Q}-\mathbf{k}}^T)\cos^2 \theta, \\
C_{\mathbf{k}} &= \frac{1}{2}(J_{\mathbf{Q}+\mathbf{k}}^T - J_{\mathbf{Q}-\mathbf{k}}^T)\sin \theta.
\end{aligned} \tag{18}$$

The coefficients $A_{\mathbf{k}}$ and $B_{\mathbf{k}}$ are even functions of \mathbf{k} , whereas $C_{\mathbf{k}}$ is an odd function of \mathbf{k} . The term \mathcal{H}_1 is linear in the bosonic operators and vanishes if the canting angle θ takes its classical value, θ_0 . The quadratic Hamiltonian is diagonalized by the Bogoliubov transformation

$$\begin{aligned}
\phi_{\mathbf{k}} &= u_{\mathbf{k}}\gamma_{\mathbf{k}} + v_{\mathbf{k}}\gamma_{-\mathbf{k}}^\dagger, \\
\phi_{-\mathbf{k}}^\dagger &= v_{\mathbf{k}}\gamma_{\mathbf{k}} + u_{\mathbf{k}}\gamma_{-\mathbf{k}}^\dagger,
\end{aligned} \tag{19}$$

where

$$\begin{aligned}
u_{\mathbf{k}}^2 &= 1 + v_{\mathbf{k}}^2 = \frac{1}{2} \left(\frac{A_{\mathbf{k}}}{\sqrt{A_{\mathbf{k}}^2 - B_{\mathbf{k}}^2}} + 1 \right), \\
u_{\mathbf{k}}v_{\mathbf{k}} &= \frac{1}{2} \frac{-B_{\mathbf{k}}}{\sqrt{A_{\mathbf{k}}^2 - B_{\mathbf{k}}^2}}.
\end{aligned} \tag{20}$$

The diagonal form of the quadratic Hamiltonian is

$$\begin{aligned}
\mathcal{H}_2 &= NS \left(J_{\mathbf{Q}}^T + (J_0^T - J_{\mathbf{Q}}^T)\sin^2 \theta - \frac{h^a}{2} \sin \theta \right) \\
&\quad + 2S \sum_{\mathbf{k}} \Omega_{\mathbf{k}} \left(\gamma_{\mathbf{k}}^\dagger \gamma_{\mathbf{k}} + \frac{1}{2} \right),
\end{aligned} \tag{21}$$

where $\Omega_{\mathbf{k}} = \sqrt{A_{\mathbf{k}}^2 - B_{\mathbf{k}}^2} + C_{\mathbf{k}}$ is the spinwave dispersion relation.^{23,24} Setting $\theta = \theta_0$, the spectrum has a gapless mode at $\mathbf{k} = 0$ as a result of the U(1) symmetry. The low-lying excitations are spin oscillations within the plane of the cycloid. For an SU(2) symmetric Hamiltonian, a second Goldstone mode is present at the ordering wave vector \mathbf{Q} of the cycloid. The low-lying excitations in this case involve oscillations of the orientation of the plane of the cycloid. For the Hamiltonian we are concerned with, the DM interaction lifts the SU(2) symmetry and generates an excitation gap at wave vector \mathbf{Q} , which becomes wider in an applied magnetic field. Recently, it has been shown that the spin-wave spectrum of an antiferromagnet in a strong magnetic field is kinematically unstable to two-magnon decay.³⁰ Here we neglect such decay processes and retain only harmonic terms in the Hamiltonian.

The ground-state energy, omitting terms $\mathcal{O}(S^0)$ and higher, is then

$$\begin{aligned}
E \equiv \langle \mathcal{H} \rangle &= NS(S+1)[J_{\mathbf{Q}}^T + (J_0^T - J_{\mathbf{Q}}^T)\sin^2 \theta] \\
&\quad - NS(S+1/2)h^a \sin \theta + S \sum_{\mathbf{k}} \Omega_{\mathbf{k}}.
\end{aligned} \tag{22}$$

The ordering wave vector is to be determined by minimizing E with respect to \mathbf{Q} . Following this procedure, the $1/S$ cor-

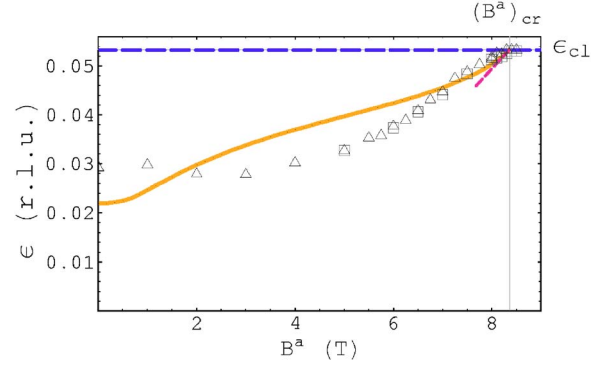


FIG. 3. (Color online) The incommensuration ϵ as a function of transverse magnetic field strength B^a . Full line: result from $1/S$ expansion. Long dashed line: result from the classical theory. Short dashed line: linear variation of ϵ with B^a , from calculation for dilute Bose gas of spin flips. Symbols are the experimental results taken from Fig. 3(c) of Ref. 3 taken at $T=0.20$ K: \triangle from magnetic Bragg peaks at $\mathbf{Q}=(0, 1.5-\epsilon, 0)$, and \square from peaks at $\mathbf{Q}=(0, 0.5-\epsilon, 1)$.

rection to E comes not only from the zero-point fluctuations but also from the renormalization of θ and \mathbf{Q} .

Results for $\mathbf{Q} \equiv (0, \frac{1}{2} + \epsilon, 0)$ to $\mathcal{O}(S^{-1})$ are shown in Fig. 3, together with data from Ref. 3. At the critical field h_{cr}^a we find, in agreement with the experiment, that \mathbf{Q} takes the classical value \mathbf{Q}_{cl} , which is field independent. This is a consequence of the fact that the ferromagnetically polarized state is an exact eigenstate of the Hamiltonian with vanishing zero-point energy. At lower fields, fluctuations renormalize \mathbf{Q} , which decreases with decreasing field: the zero-field value of the incommensuration $\epsilon=0.021$ is significantly reduced from its value at the critical field. This reduction can be understood on the basis that zero-point energy in antiferromagnets generally is lowered for states with collinear spins. The states we are concerned with are close to the collinear state with $\mathbf{Q}=(0, \frac{1}{2}, 0)$, but have lower classical energies. With decreasing field, quantum fluctuations are enhanced and drive the incommensurate wave vector towards the commensurate value. As a technical aside, we note that calculations are simplified by the presence of DM interactions, since without them the Goldstone mode at wave vector \mathbf{Q} , which appears as $\hbar \rightarrow 0$, necessitates a self-consistent treatment of quantum fluctuations.

The ordered moment is reduced from its classical value by quantum fluctuations. At leading order

$$\langle S \rangle \equiv \langle S_{\mathbf{R}}^z \rangle = S - \frac{1}{N} \sum_{\mathbf{k}} \langle \phi_{\mathbf{k}}^\dagger \phi_{\mathbf{k}} \rangle = S - \frac{1}{N} \sum_{\mathbf{k}} \frac{1}{2} \left(\frac{A_{\mathbf{k}}}{\sqrt{A_{\mathbf{k}}^2 - B_{\mathbf{k}}^2}} - 1 \right). \tag{23}$$

This is shown as a function of transverse magnetic field in Fig. 4. Our zero-field value of $\langle S \rangle = 0.25$ is close to the result $\langle S \rangle = 0.266 + \mathcal{O}(S^{-3})$ for the isotropic triangular antiferromagnet¹⁷ and to results for the anisotropic lattice without DM interactions, obtained using the $1/S$ expansion^{31,32} and series expansions.³³

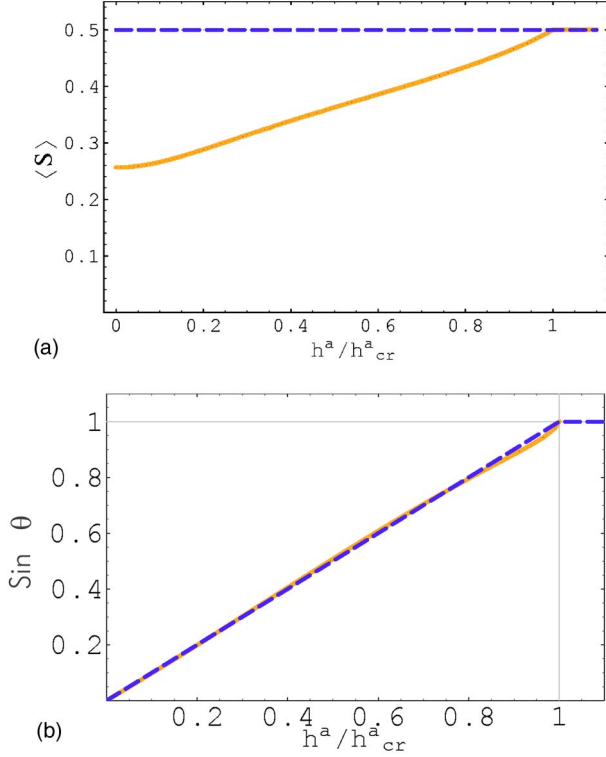


FIG. 4. (Color online) (a) The ordered moment as a function of transverse magnetic field strength. Dashed line: classical behavior; full line: with leading quantum corrections, from Eq. (23). (b) Eq. (24) is plotted as a function of the transverse field in full line, whereas $\sin \theta_0$ is plotted as a dashed line.

The canting angle θ can be determined in two different but equivalent ways. Classically, the condition $\theta = \theta_0$ ensures both that $\mathcal{H}_1 = 0$ and that $\langle \mathcal{H}_0 \rangle$ is at a minimum. The leading $1/S$ correction can be determined similarly. First, normal ordering of \mathcal{H}_3 , expressed in terms of $\gamma_{\mathbf{k}}^\dagger$ and $\gamma_{\mathbf{k}}$, yields a term linear in boson operators, which should be combined with \mathcal{H}_1 : the combination vanishes when θ takes its ground state value. Second, and alternatively, one can minimize $\langle \mathcal{H}_0 + \mathcal{H}_2 \rangle$ with respect to θ . In this way we find

$$\sin \theta = \sin \theta_0 \left[1 + \frac{1}{2SN} \sum_{\mathbf{k}} \left(\frac{A_{\mathbf{k}}}{\sqrt{A_{\mathbf{k}}^2 - B_{\mathbf{k}}^2}} - 1 \right) + \frac{1}{2SN} \sum_{\mathbf{k}} \frac{B_{\mathbf{k}}}{B_0} \sqrt{\frac{A_{\mathbf{k}} - B_{\mathbf{k}}}{A_{\mathbf{k}} + B_{\mathbf{k}}}} \right], \quad (24)$$

where $A_{\mathbf{k}}$ and $B_{\mathbf{k}}$ should be evaluated at θ_0 . Because quantum fluctuations are suppressed as the critical field is approached, $\theta \rightarrow \theta_0$ as $h^a \rightarrow h_{cr}^a$. As seen in the inset of Fig. 4, the quantum corrections to $\sin \theta$ are small and Eq. (24) is nearly equal to the unrenormalized function $\sin \theta_0 (= h^a/h_{cr}^a)$.

Combining results for the ordered moment and the canting angle, the magnetization is given by

$$m^a = \frac{g^a \mu_B}{N} \sum_{\mathbf{R}} \langle S_{\mathbf{R}}^a \rangle = g^a \mu_B \langle S_{\mathbf{R}}^z \rangle \sin \theta, \quad (25)$$

which yields

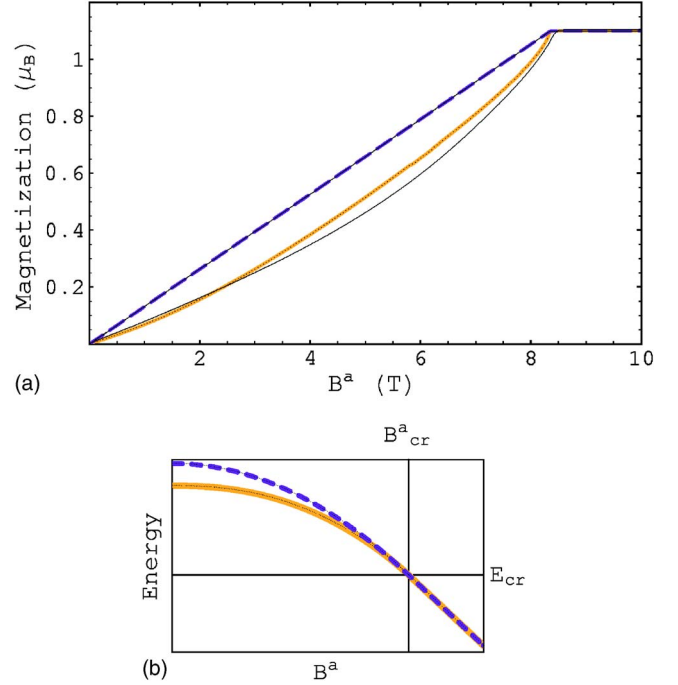


FIG. 5. (Color online) (a) The magnetization as a function of transverse magnetic field strength. The dashed line shows the result of classical theory. The thick, full line includes the $1/S$ correction from Eq. (26). The thin, full line gives experimental data (Ref. 34) measured at $T=60$ mk. (b) Calculated ground state energy as a function of transverse magnetic field. The dashed and thick lines are the results of classical theory and the $1/S$ correction, Eq. (22), respectively.

$$m^a = \frac{(g^a \mu_B)^2 B^a}{2(J_0^T - J_Q^T)} \left[1 + \frac{1}{2SN} \sum_{\mathbf{k}} \frac{B_{\mathbf{k}}}{B_0} \sqrt{\frac{A_{\mathbf{k}} - B_{\mathbf{k}}}{A_{\mathbf{k}} + B_{\mathbf{k}}}} \right] \quad (26)$$

for $h^a < h_{cr}^a$, and $m^a = g^a \mu_B S$ for $h^a > h_{cr}^a$. The $1/S$ correction on the right-hand side of Eq. (26) has a dependence on the magnetic field through the values of $A_{\mathbf{k}}$ and $B_{\mathbf{k}}$ (which again should be evaluated at θ_0). The departure of the magnetization curve from the simple linear dependence expected classically is hence a consequence of zero-point fluctuations. To understand the sign of this departure, it is useful to recall that the ground-state energy $E(B^a)$ as a function of field is related to the magnetization $m^a(B^a)$ via

$$E(0) - E(B_{cr}^a) = N \int_0^{B_{cr}^a} m^a(B^a) dB^a. \quad (27)$$

Now, since fluctuations reduce $E(0)$ below its classical value but do not contribute to $E(B_{cr}^a)$, the fluctuation contribution to Eq. (27) is negative. Supposing this to be true not only for the integral but also for the integrand at all B^a , it is natural to expect the magnetization curve at finite S to lie below the classical one for all $B^a < B_{cr}^a$. A comparison between our results and experimental data, presented in Fig. 5, shows a very good agreement.

The component S^T of the ordered moment in the plane perpendicular to the applied field can also be evaluated within the $1/S$ expansion. Defining it by

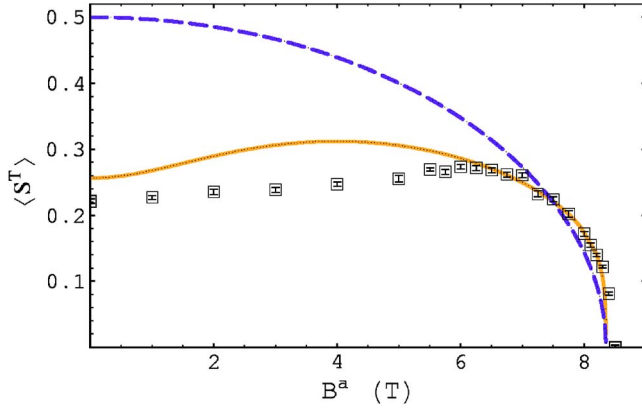


FIG. 6. (Color online) The component of ordered moment S^T in the plane perpendicular to the field direction, as a function of transverse magnetic field strength. Dashed line: classical theory. Full line: result including $1/S$ corrections, from Eq. (29). \square : experimental data at $T < 0.1$ K [taken from Fig. 3(b) of Ref. 3].

$$S^T = |\langle \mathbf{S}_R - \hat{\mathbf{a}} \langle S_R^a \rangle | \quad (28)$$

we find $S^T = \langle S \rangle \cos \theta$. Using Eqs. (23) and (24), we obtain at first order in $1/S$

$$S^T = S \cos \theta_0 \left[1 - \frac{\sec^2 \theta_0}{2SN} \sum_{\mathbf{k}} \left(\frac{A_{\mathbf{k}}}{\sqrt{A_{\mathbf{k}}^2 - B_{\mathbf{k}}^2}} - 1 \right) - \frac{\tan^2 \theta_0}{2SN} \sum_{\mathbf{k}} \frac{B_{\mathbf{k}}}{B_0} \sqrt{\frac{A_{\mathbf{k}} - B_{\mathbf{k}}}{A_{\mathbf{k}} + B_{\mathbf{k}}}} \right]. \quad (29)$$

Results are presented in Fig. 6. While classical theory gives $S^T \propto [1 - (B^a/B_{cr}^a)^2]^{1/2}$, fluctuations generate a non-monotonic dependence of S^T on B^a at low fields. This behavior can be understood on the basis that polarization of the spins with increasing applied field has the effect of reducing the phase space available for quantum fluctuations, and hence increases order. Experimental data are also shown in Fig. 6: since the absolute scale for S^T has not been determined, we scale the data to fit theory at high fields. The result of the $1/S$ expansion compares favorably to the experimental data, which also shows that at low field the perpendicular ordered moment increases with increasing field.

2. Longitudinal field

In a longitudinal field, calculations of fluctuation effects using the $1/S$ expansion are complicated by the fact that the classical ground state contains many Fourier harmonics. At low transverse fields, the classical ground state consists of a distorted cycloid in which spins lie within the b - c plane, as described in Sec. III. In this regime we write $\mathbf{S}_R = S(0, \cos \phi_R, \sin \phi_R)$ and consider the leading anharmonic distortion to the cycloid structure,^{20,28}

$$\phi_R = \mathbf{Q} \cdot \mathbf{R} + \beta \cos \mathbf{Q} \cdot \mathbf{R}, \quad (30)$$

where, for concreteness, the field is taken to be along the c axis. The distortion of the cycloid is parametrized by β : its value, determined by minimizing the classical energy, is

$$\beta = \frac{h^c}{J_{2Q}^T + J_0^T - 2J_Q^T}. \quad (31)$$

We consider quantum fluctuations about this classical state, using the Holstein-Primakoff transformation and omitting terms $\mathcal{O}([h^c]^3)$ and $\mathcal{O}(S^0)$ to obtain the Hamiltonian

$$\mathcal{H} = \mathcal{H}_0 + \mathcal{H}_2, \quad (32)$$

with

$$\mathcal{H}_0 = NS^2 \left(J_Q^T - \frac{(h^c)^2}{4(J_{2Q}^T + J_0^T - 2J_Q^T)} \right) \quad (33)$$

and

$$\begin{aligned} \mathcal{H}_2 = & NSJ_Q^T + S \sum_{\mathbf{k}} [A'_{\mathbf{k}}(\phi_{\mathbf{k}}^\dagger \phi_{\mathbf{k}} + \phi_{\mathbf{k}} \phi_{\mathbf{k}}^\dagger) + B'_{\mathbf{k}}(\phi_{-\mathbf{k}}^\dagger \phi_{\mathbf{k}}^\dagger + \phi_{-\mathbf{k}} \phi_{\mathbf{k}})] \\ & + \frac{iS\beta}{2} \sum_{\mathbf{k}} [L_{\mathbf{k}}(\phi_{\mathbf{k}} \phi_{-\mathbf{k}+\mathbf{Q}} - \phi_{-\mathbf{k}} \phi_{\mathbf{k}-\mathbf{Q}} - \text{H.c.}) \\ & + [L_{\mathbf{k}} + J_{2Q}^T - J_Q^T](\phi_{\mathbf{k}}^\dagger \phi_{\mathbf{k}-\mathbf{Q}} - \phi_{-\mathbf{k}}^\dagger \phi_{\mathbf{k}-\mathbf{Q}} - \text{H.c.})]. \end{aligned} \quad (34)$$

Here

$$\begin{aligned} A'_{\mathbf{k}} = & \frac{1}{4}(2J_{\mathbf{k}} + J_{\mathbf{Q}+\mathbf{k}}^T + J_{\mathbf{Q}-\mathbf{k}}^T) \\ & - J_Q^T + \beta^2 \left(\frac{J_{2Q+\mathbf{k}}^T + J_{2Q-\mathbf{k}}^T + J_{\mathbf{k}}^T + J_{-\mathbf{k}}^T}{16} - \frac{J_{\mathbf{Q}+\mathbf{k}}^T + J_{\mathbf{Q}-\mathbf{k}}^T}{8} \right), \end{aligned} \quad (35)$$

$$\begin{aligned} B'_{\mathbf{k}} = & \frac{1}{4}[2J_{\mathbf{k}} - J_{\mathbf{Q}+\mathbf{k}}^T - J_{\mathbf{Q}-\mathbf{k}}^T] \\ & - \beta^2 \left(\frac{J_{2Q+\mathbf{k}}^T + J_{2Q-\mathbf{k}}^T + J_{\mathbf{k}}^T + J_{-\mathbf{k}}^T}{16} - \frac{J_{\mathbf{Q}+\mathbf{k}}^T + J_{\mathbf{Q}-\mathbf{k}}^T}{8} \right), \end{aligned} \quad (36)$$

$$\begin{aligned} L_{\mathbf{k}} = & \frac{1}{8}(-J_{3Q-\mathbf{k}}^T + J_{-3Q+\mathbf{k}}^T - 2J_{2Q+\mathbf{k}}^T - J_{\mathbf{Q}+\mathbf{k}}^T \\ & - J_{-\mathbf{Q}-\mathbf{k}}^T + 2J_{-\mathbf{k}}^T + 2J_{-\mathbf{Q}+\mathbf{k}}^T). \end{aligned} \quad (37)$$

The higher Fourier harmonics in the classical ground state scatter spin fluctuations with a momentum transfer which is a multiple of \mathbf{Q} . The presence of these scattering terms, proportional to β , in the quadratic spin wave Hamiltonian means that the dispersion relation is determined by an infinite set of coupled equations.³⁵ Since our calculation is anyway restricted to small $h^c \propto \beta$, we treat these coupled equations to $\mathcal{O}(\beta^2)$ in a calculation of the ground state energy. More specifically, it is convenient first to perform a Bogoliubov transformation to diagonalize the momentum conserving terms, and then to evaluate the contribution from the terms scattering by $\pm \mathbf{Q}$ using perturbation theory. We find

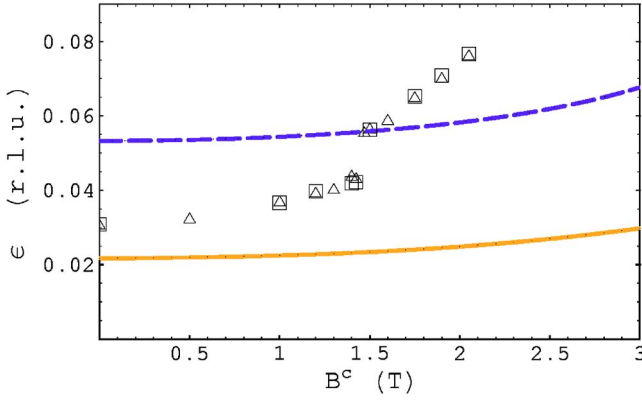


FIG. 7. (Color online) The incommensuration ϵ as a function of longitudinal field strength. Solid line: result from $1/S$ expansion, from Eq. (38). Dashed line: result from the classical result. Symbols are the experimental results taken from Ref. 2, Fig. 1(e): Δ from magnetic peaks at $\mathbf{Q}=(2, 1/2+\epsilon, 0)$ and \square from peaks at $\mathbf{Q}=(1, 1/2+\epsilon, 0)$. Experimentally, a distorted cycloid occurs for $B^c < 1.4$ T and a second incommensurate phase occurs for fields in the range $1.4 \text{ T} < B^c < 2.1 \text{ T}$.

$$E = NS(S+1)J_{\mathbf{Q}}^T - \frac{NS^2(\hbar^c)^2}{4(J_{2\mathbf{Q}}^T + J_{\mathbf{0}}^T - 2J_{\mathbf{Q}}^T)} + S \sum_{\mathbf{k}} \Omega'_{\mathbf{k}} - S\beta^2 \sum_{\mathbf{k}} \frac{2|I_{\mathbf{k}}|^2}{\Omega'_{\mathbf{k}} + \Omega'_{\mathbf{Q}-\mathbf{k}}}, \quad (38)$$

with $\Omega'_{\mathbf{k}} = \sqrt{(A'_{\mathbf{k}})^2 - (B'_{\mathbf{k}})^2}$ and

$$I_{\mathbf{k}} = -\frac{i}{2} [L_{\mathbf{k}}(u'_{\mathbf{k}} - v'_{\mathbf{k}})(u'_{\mathbf{Q}-\mathbf{k}} - v'_{\mathbf{Q}-\mathbf{k}}) - (J_{2\mathbf{Q}}^T - J_{\mathbf{Q}}^T)(u'_{\mathbf{k}}v'_{\mathbf{Q}-\mathbf{k}} + v'_{\mathbf{k}}u'_{\mathbf{Q}-\mathbf{k}})], \quad (39)$$

where $u'_{\mathbf{k}}$ and $v'_{\mathbf{k}}$ are given by Eq. (20) after substituting $A'_{\mathbf{k}}$ and $B'_{\mathbf{k}}$ for $A_{\mathbf{k}}$ and $B_{\mathbf{k}}$.

The ordering wave vector and its dependence on field can be calculated by minimizing Eq. (38) with respect to \mathbf{Q} . It is interesting to note that, in contrast to the case for a transverse field, the ordering wave vector in a longitudinal field is dependent on field strength even at the classical level. It increases with field and this trend is reinforced by the quantum fluctuations. Results are shown in Fig. 7, together with experimental data. The observed increase of \mathbf{Q} with field is much faster than the calculated one; the origin of this discrepancy is not understood.

Now we turn to the case of stronger longitudinal fields. In the field range $0.35 < \hbar^c/\hbar_{cr}^c < 1$, the classical treatment described in Sec. III gives the tilted cone of Eq. (12) as the ground state. The tilting angle η of the cone axis from the field direction is given approximately by $\tan \eta \approx (D/\hbar_{cr}^c)[1 - (\hbar_{cr}^c/\hbar^c)^2]$ and is less than 1 deg for $\hbar^c > 0.9\hbar_{cr}^c$. Experimentally, an incommensurately ordered state has recently been observed⁵ for $7.1 \text{ T} < B^c < B_{cr}^c$. With this in mind, we approximate the classical ground state in this field range by setting $\eta=0$ in Eq. (12) and use the $1/S$ expansion to study the effects of quantum fluctuations. Following a procedure similar to the one described for a transverse field, we have

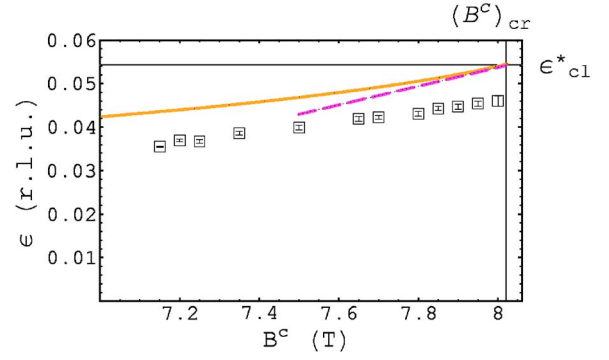


FIG. 8. (Color line) The incommensuration ϵ as a function of longitudinal magnetic field strength B^c . Solid line: result from $1/S$ expansion. Dashed line: result from calculation for dilute Bose gas of reversed spins. \square : experimental data (Ref. 5) (no incommensurate ordering is observed for $2.1 \text{ T} < B^c < 7.1 \text{ T}$).

calculated the ordering wave vector as a function of field. While the observed phase has not so far been fully characterized, its ordering wave vector has been measured as a function of field strength. From our classical calculation, we expect the state to be a tilted cone. Our results for the ordering wave vector are compared with experimental data in Fig. 8. Calculated and observed values of the ordering wave vector vary in the same way with field, but there is an offset between the two which remains a puzzle. In the following subsection IV B, we obtain results that are essentially exact close to B_{cr}^c . Since the discrepancy remains, we conclude that the value of the ordering wave vector is influenced by interactions not included in the model Hamiltonian of Eq. (1).

B. Dilute Bose gas

An alternative to the $1/S$ expansion can be motivated by noting that fully polarized states are exact eigenstates of the Hamiltonian. The absence of quantum fluctuations suggests a systematic expansion in powers of the density of reversed spins,^{36–38} equivalent to an expansion in powers of $(1 - \hbar/\hbar_{cr})$. In this approach reversed spins constitute a dilute gas of bosons with hard-core repulsion.

1. Transverse field

We introduce boson creation and annihilation operators, $\phi_{\mathbf{R}}^{\dagger}$ and $\phi_{\mathbf{R}}$, to represent spins, setting, for a transverse field,

$$S_{\mathbf{R}}^a = \frac{1}{2} - \phi_{\mathbf{R}}^{\dagger} \phi_{\mathbf{R}},$$

$$S_{\mathbf{R}}^+ = S_{\mathbf{R}}^b + iS_{\mathbf{R}}^c = \phi_{\mathbf{R}}, \quad (40)$$

$$S_{\mathbf{R}}^- = S_{\mathbf{R}}^b - iS_{\mathbf{R}}^c = \phi_{\mathbf{R}}^{\dagger}$$

with the constraint that the particle number $n_{\mathbf{R}} = \phi_{\mathbf{R}}^{\dagger} \phi_{\mathbf{R}}$ takes only the values 0 and 1. This is imposed by introducing an on-site interaction U and taking the limit $U \rightarrow \infty$.

The Hamiltonian for a single layer (with, for definiteness, the layer index n chosen to be even) is

$$\mathcal{H} = N \left[\frac{J_0 - h^a}{4} \right] + \sum_{\mathbf{k}} (\epsilon_{\mathbf{k}}^T - \mu) \phi_{\mathbf{k}}^\dagger \phi_{\mathbf{k}} + \frac{1}{2N} \sum_{\mathbf{k}, \mathbf{k}', \mathbf{q}} V_{\mathbf{q}}(\mathbf{k}, \mathbf{k}') \phi_{\mathbf{k}+\mathbf{q}}^\dagger \phi_{\mathbf{k}'-\mathbf{q}}^\dagger \phi_{\mathbf{k}'} \phi_{\mathbf{k}}, \quad (41)$$

where

$$\epsilon_{\mathbf{k}}^T = J_{\mathbf{k}}^T - J_{\mathbf{Q}}^T, \quad (42)$$

$$\mu = \frac{h_{cr}^a - h^a}{2}, \quad (43)$$

$$V_{\mathbf{q}}(\mathbf{k}, \mathbf{k}') = 2J_{\mathbf{q}} + 2U. \quad (44)$$

Standard techniques³⁹ developed for the interacting Bose gas can be applied to treat this Hamiltonian. For $h^a > h_{cr}^a$ the spin system is fully polarized. Equivalently, for $\mu < 0$ the ground state is the boson vacuum. Conservation of boson number follows from U(1) symmetry of the spin Hamiltonian in a transverse field. Magnetic order of in-plane spin components below the critical field translates, using Eq. (40), to formation of a Bose condensate for $\mu > 0$. We introduce the order parameter $\psi_{\mathbf{q}}$ and shift the boson annihilation operator by a constant

$$\phi_{\mathbf{Q}} \rightarrow \sqrt{N} \psi_{\mathbf{Q}} + \phi_{\mathbf{Q}}, \quad (45)$$

where the ordering wave vector \mathbf{Q} need not take the classical value \mathbf{Q}_{cl} . Minimization of the ground-state energy is equivalent to requiring $\langle \phi_{\mathbf{Q}} \rangle = 0$. Working in the low density limit, the scattering amplitude between bosons is given by an effective interaction potential $\Gamma_{\mathbf{q}}(\mathbf{k}, \mathbf{k}')$ which results from summing ladder diagrams. It satisfies the integral equation

$$\Gamma_{\mathbf{q}}(\mathbf{k}, \mathbf{k}') = V_{\mathbf{q}} - \frac{1}{N} \sum_{\mathbf{q}'} \frac{V_{\mathbf{q}-\mathbf{q}'}}{\epsilon_{\mathbf{k}+\mathbf{q}'}^T + \epsilon_{\mathbf{k}'-\mathbf{q}'}^T - \epsilon_{\mathbf{k}}^T - \epsilon_{\mathbf{k}'}^T} \Gamma_{\mathbf{q}'}(\mathbf{k}, \mathbf{k}'). \quad (46)$$

The ground state energy, including the leading interaction effects at low density, is

$$E^{(2)} = N \left[\frac{J_0^T - h^a}{4} + (\epsilon_{\mathbf{Q}}^T - \mu) |\psi_{\mathbf{Q}}|^2 + \frac{1}{2} \Gamma_0(\mathbf{Q}, \mathbf{Q}) |\psi_{\mathbf{Q}}|^4 \right] + \frac{1}{2} \sum_{\mathbf{k}} (E_{\mathbf{k}} - F_{\mathbf{k}}) \quad (47)$$

where $E_{\mathbf{k}} = \sqrt{F_{\mathbf{k}}^2 - G_{\mathbf{k}}^2} + N_{\mathbf{k}}$, and

$$F_{\mathbf{k}} = \frac{\epsilon_{\mathbf{Q}+\mathbf{k}}^T + \epsilon_{\mathbf{Q}-\mathbf{k}}^T}{2} - \mu + \frac{|\psi_{\mathbf{Q}}|^2}{2} [\Gamma_{\mathbf{k}}(\mathbf{Q}, \mathbf{Q} + \mathbf{k}) + \Gamma_{-\mathbf{k}}(\mathbf{Q} + \mathbf{k}, \mathbf{Q}) + \Gamma_0(\mathbf{Q}, \mathbf{Q} + \mathbf{k}) + \Gamma_0(\mathbf{Q} + \mathbf{k}, \mathbf{Q})],$$

$$G_{\mathbf{k}} = |\psi_{\mathbf{Q}}|^2 \Gamma_{\mathbf{k}}(\mathbf{Q}, \mathbf{Q}),$$

$$N_{\mathbf{k}} = \frac{\epsilon_{\mathbf{Q}+\mathbf{k}}^T - \epsilon_{\mathbf{Q}-\mathbf{k}}^T}{2}. \quad (48)$$

The condition $\langle \phi_{\mathbf{Q}} \rangle = 0$ yields an expression for the order parameter

$$|\psi_{\mathbf{Q}}|^2 = \frac{\mu - \epsilon_{\mathbf{Q}}^T}{\Gamma_0(\mathbf{Q}, \mathbf{Q})}. \quad (49)$$

Substituting this into Eq. (47), the ground-state energy is

$$E^{(2)} = N \left[\frac{J_0^T}{4} - \frac{h^a}{4} - \frac{(\mu - \epsilon_{\mathbf{Q}}^T)^2}{2\Gamma_0(\mathbf{Q}, \mathbf{Q})} \right] + \frac{1}{2} \sum_{\mathbf{k}} (E_{\mathbf{k}} - F_{\mathbf{k}}).$$

As in the $1/S$ calculation, the ordering wave vector can be determined as a function of field by minimizing $E^{(2)}$ with respect to \mathbf{Q} . Our focus here, however, is on exact results close to the critical field. At $h^a = h_{cr}^a$, we find $\mathbf{Q} = \mathbf{Q}_{cl}$. In addition, we obtain

$$\left. \frac{\partial \mathbf{Q}}{\partial h^a} \right|_{h^a=h_{cr}^a} = \frac{1}{4} \hat{\mathbf{k}} \left(\frac{\partial^3 E^{(2)}}{\partial Q_k^2 \partial \mu} \right)^{-1} \left. \frac{\partial^3 E^{(2)}}{\partial Q_k \partial \mu^2} \right|_{h^a=h_{cr}^a, \mathbf{Q}=\mathbf{Q}_{cl}}$$

and hence

$$\left. \frac{\partial \mathbf{Q}}{\partial h^a} \right|_{h^a=h_{cr}^a} = \frac{1}{4} \hat{\mathbf{k}} \left(\frac{\partial^2 \epsilon_{\mathbf{Q}}^T}{\partial Q_k^2} \right)^{-1} \frac{\partial}{\partial Q_k} \ln \left[\frac{1}{\Gamma_0(\mathbf{Q}, \mathbf{Q})} + \frac{1}{N} \sum_{\mathbf{k}} \frac{1}{\epsilon_{\mathbf{Q}+\mathbf{k}}^T + \epsilon_{\mathbf{Q}-\mathbf{k}}^T} \left(\frac{\Gamma_{\mathbf{k}}(\mathbf{Q}, \mathbf{Q})}{\Gamma_0(\mathbf{Q}, \mathbf{Q})} \right)^2 \right] \Bigg|_{\mathbf{Q}=\mathbf{Q}_{cl}}. \quad (50)$$

A potential difficulty arises at this point because interactions are marginally irrelevant at the critical point of the two-dimensional Bose gas:⁴⁰ in consequence, $\Gamma_0(\mathbf{Q}_{cl}, \mathbf{Q}_{cl})$ vanishes for an isolated layer. It is therefore essential to include interlayer exchange J' in the calculation of the vertex. Evaluating Eq. (50) numerically, we find $h_{cr}^a \partial \mathbf{Q} / \partial h^a = (0, 0.0911, 0)$. This result is displayed in Fig. 3: it is similar to that given by the $1/S$ expansion, indicating that the linear spinwave theory captures the effects of quantum fluctuations quite accurately in this system. Both approaches are in good agreement with experiment, especially close to the critical field.

2. Longitudinal field

A similar procedure can be followed for the system in longitudinal field [chosen along the c axis, without loss of generality for the Hamiltonian of Eq. (1)]. With this field orientation, the expressions for spin operators in terms of Bose operators are

$$\begin{aligned} S_{\mathbf{R}}^c &= \frac{1}{2} - \phi_{\mathbf{R}}^\dagger \phi_{\mathbf{R}}, \\ S_{\mathbf{R}}^+ &= S_{\mathbf{R}}^a + i S_{\mathbf{R}}^b = \phi_{\mathbf{R}}, \\ S_{\mathbf{R}}^- &= S_{\mathbf{R}}^a - i S_{\mathbf{R}}^b = \phi_{\mathbf{R}}^\dagger. \end{aligned} \quad (51)$$

The Hamiltonian for a single layer (again taking the layer index n to be even) is

$$\begin{aligned} \mathcal{H} = & N \left[\frac{J_0 - h^c}{4} \right] + \sum_{\mathbf{k}} (\epsilon_{\mathbf{k}}^L - \mu) \phi_{\mathbf{k}}^\dagger \phi_{\mathbf{k}} \\ & + \frac{1}{2\sqrt{N}} \sum_{\mathbf{k}, \mathbf{k}'} (D_{\mathbf{k}} + D_{\mathbf{k}'}) (\phi_{\mathbf{k}+\mathbf{k}'}^\dagger \phi_{\mathbf{k}'} \phi_{\mathbf{k}} + \text{H.c.}) \\ & + \frac{1}{2N} \sum_{\mathbf{k}, \mathbf{k}', \mathbf{q}} V_{\mathbf{q}}(\mathbf{k}, \mathbf{k}') \phi_{\mathbf{k}+\mathbf{q}}^\dagger \phi_{\mathbf{k}'-\mathbf{q}}^\dagger \phi_{\mathbf{k}'} \phi_{\mathbf{k}}, \end{aligned} \quad (52)$$

where

$$\epsilon_{\mathbf{k}}^L - \mu = J_{\mathbf{k}} - J_0 + h^c/2. \quad (53)$$

The presence of a term cubic in boson operators considerably complicates the analysis, since with it, particle number is not conserved. Its appearance reflects the fact that a longitudinal field breaks $U(1)$ symmetry as discussed in Sec. II. In general, the particle number (or longitudinal magnetization) is not conserved (except for the boson vacuum—the ferromagnetic state—which is an exact eigenstate of the Hamiltonian). The remaining, \mathbb{Z}_2 symmetry is invariant under the canonical transformation $\phi_{\mathbf{k}}^\dagger \rightarrow -\phi_{-\mathbf{k}}^\dagger$.

We note in passing that the cubic term does not result in a first-order transition from the fully polarized state as μ is varied, because momentum conservation precludes contributions involving only the ordering fields $\phi_{\mathbf{Q}}$ and $\phi_{-\mathbf{Q}}$ in a Landau-Ginzburg description. An ordered state is therefore brought about by the closing of the single-particle excitation gap, yielding a second-order phase transition. The universality class associated with this quantum phase transition must take into account the extra \mathbb{Z}_2 symmetry of the Hamiltonian. The low energy action is described by a $\mathbb{Z}_2 \oplus U(1)$ symmetry model. This multicritical transition found in longitudinal field is to be contrasted with the ordinary XY quantum phase transition found in transverse field.⁴¹

While for a transverse field the ordering wave vector can be found simply from the quadratic part of the boson Hamiltonian, this is not so for a longitudinal field. In that case, because particle number is not conserved, the quasiparticle spectrum is renormalized by quantum fluctuations, even at the critical point. It is interesting to check whether a renormalization of this kind may be responsible for the discrepancy between theory and experiment shown in Fig. 8. The critical field and the ordering wave vector are determined from the values of h^c and \mathbf{Q} for which the one-particle Green function has a pole at zero energy, by solving

$$G(\mathbf{Q}, E_{\mathbf{Q}} = 0)^{-1} = 0. \quad (54)$$

In absence of DM interactions, the one-particle Green function at and above the critical field is given exactly at zero temperature by the expression for a noninteracting system, $G^0(\mathbf{k}, i\omega) = (i\omega - \epsilon_{\mathbf{k}}^L + \mu)^{-1}$. Since $D \ll J$, we evaluate the leading contribution to the self-energy,

$$\Sigma(\mathbf{k}, i\omega) = \frac{1}{2N} \sum_{\mathbf{q}} \frac{[D_{(\mathbf{k}+\mathbf{q})/2} + D_{(\mathbf{k}-\mathbf{q})/2}]^2}{i\omega - \epsilon_{(\mathbf{k}+\mathbf{q})/2}^L - \epsilon_{(\mathbf{k}-\mathbf{q})/2}^L + 2\mu} + \mathcal{O}(D^4), \quad (55)$$

yielding a renormalized quasiparticle spectrum $\omega_{\mathbf{k}} \approx \epsilon_{\mathbf{k}}^L - \mu + \Sigma(\mathbf{k}, \epsilon_{\mathbf{k}}^L - \mu)$ in the symmetric phase. The ordering wave

vector can be found by solving Dyson's equation at the critical field,

$$G^0(\mathbf{Q}, 0)^{-1} - \Sigma(\mathbf{Q}, 0) = 0, \quad (56)$$

which gives $\mathbf{Q} = \mathbf{Q}_{cl}^* + (0, 0.00025, 0)$. This minute quantum correction at the critical field is nearly two orders of magnitude too small to explain the discrepancy between \mathbf{Q}_{cl}^* and the experimental ordering wave vector illustrated in Fig. 8. We conclude that there are further anisotropic interactions present in the system but not captured by the Hamiltonian of Eq. (1). Additional evidence for this is provided by the fact that the experimental phase diagram in a longitudinal field depends on field orientation *within* the b - c plane.⁵

It is interesting to note that at the critical point in a longitudinal field, in contrast to behavior for a transverse field, order is possible at two wave vectors, $\pm\mathbf{Q}$. Cone states break spontaneously the Ising symmetry, with condensation either at \mathbf{Q} or at $-\mathbf{Q}$. An alternative possibility is the *simultaneous* condensation of magnons at both wave vectors, forming a fan phase. Competition between the fan and cone phases is determined by the interaction between magnons. A straightforward calculation shows that the cone phase is favored if

$$\Gamma_0(\mathbf{Q}, \mathbf{Q}) < \Gamma_0(\mathbf{Q}, -\mathbf{Q}) + \Gamma_{2\mathbf{Q}}(\mathbf{Q}, -\mathbf{Q}), \quad (57)$$

while the fan phase is preferred if the inequality is reversed. Evaluating the vertices numerically, we find that, although quantum fluctuations renormalize interactions, they do not modify the character of the ground state found from the classical calculation, and the cone state is favored.

V. INTERLAYER COUPLING

To this point, we have omitted the interlayer coupling J'' [except where it was essential, in order to obtain a nonzero value for the interaction vertex $\Gamma_{\mathbf{q}}(\mathbf{k}, \mathbf{k}')$]. It is relatively weak ($J''/J \approx 0.05$), though crucial in stabilizing long-range order against thermal fluctuations. As well as being small, it is also frustrated by DM interactions, because the sign of the DM interactions alternates between layers [see Eq. (3)]. The frustration introduces distortions in the cone states, which we discuss in this section.

More specifically, considering zero field for simplicity, the classical ground state in the absence of interlayer coupling consists of a spin spiral with wave vector $+\mathbf{Q}$ in layers with even index n , and wave vector $-\mathbf{Q}$ in odd layers, as in Eq. (10). By contrast, for a system with antiferromagnetic interlayer exchange but no DM interactions, the ground state consists of spin spirals with the same wave vector (say $+\mathbf{Q}$) in every layer, and with alternating phases α in even and odd layers, so that

$$\mathbf{S}_{\mathbf{R}} = \begin{pmatrix} 0 \\ \cos(\mathbf{Q} \cdot \mathbf{R} + n\pi) \\ \sin(\mathbf{Q} \cdot \mathbf{R} + n\pi) \end{pmatrix}. \quad (58)$$

With both interlayer exchange and DM interactions, their competition results in a ground state which is a superposition of the two structures.³ In the presence of a transverse field, spins lie on an elliptical cone around the field direction with

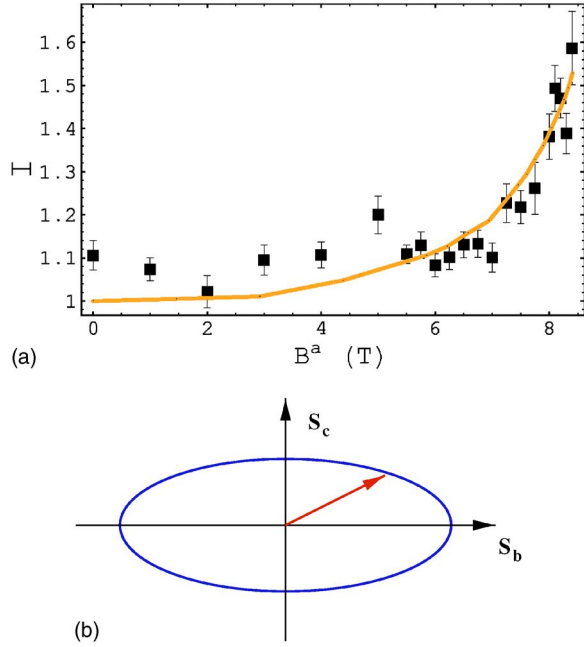


FIG. 9. (Color online) The eccentricity of ellipse $I=S_b/S_c$ as a function of the transverse magnetic field strength. Line: result of classical analysis. \square : experimental data (Ref. 5).

$$\mathbf{S}_{\mathbf{R}} = \begin{pmatrix} S_a(\mathbf{R}) \\ (-1)^n S_1 \cos \mathbf{Q} \cdot \mathbf{R} + (-1)^n S_2 \cos(-\mathbf{Q} \cdot \mathbf{R}) \\ S_1 \sin \mathbf{Q} \cdot \mathbf{R} + S_2 (\sin -\mathbf{Q} \cdot \mathbf{R}) \end{pmatrix} = \begin{pmatrix} S_a(\mathbf{R}) \\ (-1)^n S_b \cos \mathbf{Q} \cdot \mathbf{R} \\ S_c \sin \mathbf{Q} \cdot \mathbf{R} \end{pmatrix}, \quad (59)$$

where U(1) symmetry has been broken by selecting the b -component of the spin to alternate on adjacent layers. The eccentricity $I=(S_1+S_2)/(S_1-S_2)=S_b/S_c$ of the cone is a measure of the mixing of the two spin spirals at wave vectors $\pm\mathbf{Q}$.

Experimentally, this ratio can be measured by determining the relative intensity of two magnetic Bragg peaks associated with the spin ordering,⁵ the critical field, and we focus on its field dependence. The mixing between the two spin structures is observed to be particularly strong near the critical field, where it can be calculated using linear spinwave theory.³ More generally, we find the field dependence of I by minimizing the classical energy over states which are parametrized as in Eq. (59). Results (obtained numerically) compare well with experimental data, as shown in Fig. 9. Mixing is small ($I \approx 1$) in zero field, but rises rapidly near the critical field to reach the value $I=1.52$ at $B^a=B_{cr}^a$.

To gain insight into these results, it is useful to consider behavior close to the critical field, and expand in powers of the small in-plane spin components, S_b and S_c . Following this procedure we obtain to quartic order the energy

$$E = N \left(S^2(J_0 + J'' - h^a) + (J_{\mathbf{Q}} - J_0 - J'' + h^a/2)(S_b^2 + S_c^2)/2 + D_{\mathbf{Q}}S_bS_c + J''(S_c^2 - S_b^2)/2 + \frac{J_{2\mathbf{Q}} - J_0}{32S^2}(S_b^2 - S_c^2)^2 + \frac{h^a}{64S^2}(3S_b^4 + 3S_c^4 + 2S_b^2S_c^2) \right). \quad (60)$$

This should be minimized with respect to S_b and S_c . It is convenient to change variables, writing $S_b=r \sin \chi$ and $S_c=r \cos \chi$, so that

$$E = N \left\{ S^2(J_0 + J'' - h^a) + \frac{r^2}{2}(J_{\mathbf{Q}} - J_0 - J'' + h^a/2 + D_{\mathbf{Q}} \sin 2\chi + J'' \cos 2\chi) + r^4 \left[\frac{J_{2\mathbf{Q}} - J_0}{32S^2} \cos^2 2\chi + \frac{h}{64S^2}(1 + 2 \cos^4 \chi + 2 \sin^4 \chi) \right] \right\}. \quad (61)$$

The eccentricity is then $I=\tan \chi$. As the critical field is approached from below, $r \rightarrow 0^+$ and χ is determined solely by the quadratic term, yielding $\tan \chi = D_{\mathbf{Q}}/(J'' - \sqrt{(J'')^2 + (D_{\mathbf{Q}})^2}) = 1.52$, as reported previously.³ Note that the interlayer exchange modifies the previous estimate for the critical field (see Sec. III) to $h_{cr}^a = 2[J_0 - J_{\mathbf{Q}} + J'' + \sqrt{(J'')^2 + (D_{\mathbf{Q}})^2}]$, giving $B_{cr}^a = 8.51T$. With reducing field, r increases and I is determined partly by the χ dependence of the quartic term, which is minimum at $\chi = \pi/4 + m\pi/2$ (taking $h^a \gg J_{2\mathbf{Q}} - J_0$). The quartic term hence favors $|I|=1$ and dominates as h^a is reduced below h_{cr}^a .

VI. CONCLUSIONS

In summary, we have presented a detailed investigation of ground-state properties of an anisotropic triangular lattice antiferromagnet with Dzyaloshinskii-Moriya interactions, focusing on behavior in an applied magnetic field and its dependence on field direction. We have supplemented calculations for a classical model with two approaches to quantum fluctuations: one using linear spin wave theory, and the other treating reversed spins in an almost polarized state as a dilute Bose gas. We have compared our calculations with experimental data on Cs_2CuCl_4 .^{1-5,34} The outcome of this comparison depends strikingly on field direction. For a transverse field, theory is in qualitative, and on many points quantitative, agreement with experiment. For a longitudinal field, central aspects of the low-temperature phase diagram remain to be understood.

In more detail, for a transverse field the classical model yields the observed incommensurate cone state with a field-dependent canting angle. Interlayer exchange interactions influence this ordering in ways that are also well described by classical theory. However, to account for the measured field dependence of ordering wave vector, the magnetization, and the local ordered moment, it is necessary to include the effect of quantum fluctuations. Linear spin wave theory gives quite accurate results for the magnetization and qualitatively cor-

rect behavior for the other two quantities; the large reduction at low fields of the ordered moment below its classical value demonstrates the importance of fluctuations. In addition, calculations for the almost polarized system fit observations of the ordering wave vector very well, as they should since that aspect of the theory is asymptotically exact.

By contrast, for a longitudinal field there are clear differences between the phase diagram of the classical model and experiment. In this case, classical theory yields a distorted cycloid as the ground state at low fields, separated by a first-order phase transition from a tilted cone state at higher fields. Experimentally, most of the high-field region is occupied by a third phase, in which no magnetic Bragg peaks have been reported,³ although incommensurate order has recently been observed in a narrow field window below the saturation field.⁵ Focusing on the ordering wave vector of the incommensurate phases, spin wave theory gives only a mediocre account of its behavior at low field, while neither spin wave theory nor calculations for the almost polarized system can explain its value close to saturation. In this connection, it is worth emphasizing that the model Hamiltonian we have used must in fact omit some residual interactions which are of importance, since it is invariant under rotations of the magnetic field about the a direction, while the observed phase diagram does not have exactly this symmetry.⁵

For the future, the nature of the ground state in a longitudinal field at intermediate field strengths remains an intriguing problem, which we intend to address elsewhere.⁴²

ACKNOWLEDGMENT

The work was supported by EPSRC under Grant No. GR/R83712/01 (JTC) and No. GR/R76714/01 (RC).

APPENDIX: LADDER DIAGRAM SUMMATION

In this appendix we show how we solve numerically the integral equation for the effective interaction potential, $\Gamma_{\mathbf{q}}(\mathbf{k}, \mathbf{k}')$. We recall Eq. (46),

$$\Gamma_{\mathbf{q}} = V_{\mathbf{q}} - \frac{1}{N} \sum_{\mathbf{q}'} V_{\mathbf{q}-\mathbf{q}'} n_{\mathbf{q}'} \Gamma_{\mathbf{q}'}, \quad (\text{A1})$$

where for clarity we have omitted the variables \mathbf{k}, \mathbf{k}' and introduced

$$n_{\mathbf{q}'} = \frac{1}{\epsilon_{\mathbf{k}+\mathbf{q}'} + \epsilon_{\mathbf{k}'-\mathbf{q}'} - \epsilon_{\mathbf{k}} - \epsilon_{\mathbf{k}'}}. \quad (\text{A2})$$

The bare interaction $V_{\mathbf{q}}$ arises as the Fourier transform of an interaction in real space, in the form $V_{\mathbf{q}} = \sum_{\mathbf{R}} A_{\mathbf{R}} \exp(-i\mathbf{q} \cdot \mathbf{R})$. Crucially, since the interaction is short range, only a small set of coefficients $A_{\mathbf{R}}$ are nonzero. In turn, this implies that $\Gamma_{\mathbf{q}}$ can also be expressed using a small number of Fourier coefficients, as follows. Define the parameters $B_{\mathbf{R}}$ through the equation $\Gamma_{\mathbf{q}} = \sum_{\mathbf{R}} B_{\mathbf{R}} \exp(-i\mathbf{q} \cdot \mathbf{R})$. Then from Eq. (A1) we obtain

$$B_{\mathbf{R}} = A_{\mathbf{R}} \left(1 - \sum_{\mathbf{R}'} M_{\mathbf{R},\mathbf{R}'} B_{\mathbf{R}'} \right), \quad (\text{A3})$$

with $M_{\mathbf{R},\mathbf{R}'} = (1/N) \sum_{\mathbf{q}} n_{\mathbf{q}} e^{-i\mathbf{q} \cdot (\mathbf{R}-\mathbf{R}')}$. A simple consequence of Eq. (A3) is that if $A_{\mathbf{R}} = 0$ for a given \mathbf{R} , then $B_{\mathbf{R}} = 0$ as well. From Eq. (A3) we find

$$B_{\mathbf{R}} = \sum_{\mathbf{R}'} (A^{-1} + M)_{\mathbf{R},\mathbf{R}'}^{-1}. \quad (\text{A4})$$

Since the Hamiltonian has only nearest-neighbor interactions on a stacked triangular lattice, the matrix we must invert has 9×9 elements. These can be evaluated numerically.

-
- ¹R. Coldea, D. A. Tennant, R. A. Cowley, D. F. McMorrow, B. Dorner, and Z. Tylczynski, Phys. Rev. Lett. **79**, 151 (1997).
²R. Coldea, D. A. Tennant, A. M. Tsvetik, and Z. Tylczynski, Phys. Rev. Lett. **86**, 1335 (2001).
³R. Coldea, D. A. Tennant, K. Habicht, P. Smeibidl, C. Wolters, and Z. Tylczynski, Phys. Rev. Lett. **88**, 137203 (2002).
⁴R. Coldea, D. A. Tennant, and Z. Tylczynski, Phys. Rev. B **68**, 134424 (2003).
⁵R. Coldea (unpublished).
⁶M. Bocquet, F. H. L. Essler, A. M. Tsvetik, and A. O. Gogolin, Phys. Rev. B **64**, 094425 (2001).
⁷C. H. Chung, J. B. Marston, and R. H. McKenzie, J. Phys.: Condens. Matter **13**, 5159 (2001).
⁸S.-Q. Shen and F. C. Zhang, Phys. Rev. B **66**, 172407 (2002).
⁹C.-H. Chung, K. Voelker, and Y. B. Kim, Phys. Rev. B **68**, 094412 (2003).
¹⁰J. Y. Gan, F. C. Zhang, and Z. B. Su, Phys. Rev. B **67**, 144427 (2003).
¹¹Y. Zhou and X.-G. Wen, cond-mat/0210662.
¹²P. W. Anderson, Mater. Res. Bull. **8**, 153 (1973).
¹³P. Fazekas and P. W. Anderson, Philos. Mag. **30**, 23 (1974).
¹⁴G. Misguich and C. Lhuillier, *Frustrated Spinn Systems* (World Scientific, Singapore, 2004); cond-mat/0310405.
¹⁵C. M. Canali, S. M. Girvin, and M. Wallin, Phys. Rev. B **45**, 10131 (1992).
¹⁶J. I. Igarashi, Phys. Rev. B **46**, 10763 (1992).
¹⁷A. V. Chubukov, S. Sachdev, and T. Senthil, J. Phys.: Condens. Matter **6** 8891 (1994).
¹⁸I. Dzyaloshinskii, J. Phys. Chem. Solids **4**, 241 (1958); T. Moriya, Phys. Rev. **120**, 91 (1960).
¹⁹S. Bailleul, J. Holsa, and P. Porcher, Eur. J. Solid State Inorg. Chem. **31**, 432 (1994).
²⁰T. Nagamiya, K. Nagata, and Y. Kitano, Prog. Theor. Phys. **27**, 1253 (1962).
²¹R. J. Elliot and R. V. Lange, Phys. Rev. **152**, 235 (1966).
²²A. V. Chubukov and D. I. Golosov, J. Phys.: Condens. Matter **3**, 69 (1991).
²³T. Nagamiya, *Solid State Physics*, edited by F. Seitz, D. Turnbull, and H. Ehrenreich (Academic, New York, 1967), Vol. 2, p. 305; J. Jensen and A. R. Mackintosh, *Rare Earth Magnetism. Structures and Excitations* (Clarendon, Oxford, 1991), p. 286.
²⁴R. M. White, *Quantum Theory of Magnetism* (Springer, Berlin,

- 1983).
- ²⁵T. Nikuni and H. Shiba, J. Phys. Soc. Jpn. **62**, 3268 (1993).
- ²⁶T. Ohyama and H. Shiba, J. Phys. Soc. Jpn. **62**, 3277 (1993).
- ²⁷T. Ohyama and H. Shiba, J. Phys. Soc. Jpn. **63**, 3454 (1994).
- ²⁸M. E. Zhitomirsky and I. A. Zaliznyak, Phys. Rev. B **53**, 3428 (1996).
- ²⁹M. E. Zhitomirsky and T. Nikuni, Phys. Rev. B **57**, 5013 (1998).
- ³⁰M. E. Zhitomirsky and A. L. Chernyshev, Phys. Rev. Lett. **82**, 4536 (1999).
- ³¹A. E. Trumper, Phys. Rev. B **60**, 2987 (1999).
- ³²J. Merino, R. H. McKenzie, J. B. Marston, and C. H. Chung, J. Phys.: Condens. Matter **11**, 2965 (1999).
- ³³Weihong Zheng, R. H. McKenzie, and R. R. P. Singh, Phys. Rev. B **59**, 14367 (1999).
- ³⁴Y. Tokiwa *et al.* (unpublished).
- ³⁵T. Ziman and P. A. Lindgard, Phys. Rev. B **33**, 1976 (1986).
- ³⁶E. G. Batyev and L. S. Braginskii, Sov. Phys. JETP **60**, 4 (1984).
- ³⁷S. Gluzman, Z. Phys. B: Condens. Matter **90**, 313 (1993).
- ³⁸T. Nikuni and H. Shiba, J. Phys. Soc. Jpn. **64**, 3471 (1995).
- ³⁹A. A. Abrikosov, L. P. Gorkov, and I. E. Dzyaloshinskii, in *Methods of Quantum Field Theory In Statistical Physics* (Dover, New York 1963).
- ⁴⁰D. S. Fisher and P. C. Hohenberg, Phys. Rev. B **37**, 4936 (1988).
- ⁴¹M. E. Fisher and D. R. Nelson, Phys. Rev. Lett. **32**, 1350 (1974); A. Pelissetto and E. Vicari, hep-th/0409214.
- ⁴²M. Y. Veillette and J. T. Chalker (unpublished).